Solid Freeform Fabrication 2017: Proceedings of the 28th Annual International Solid Freeform Fabrication Symposium – An Additive Manufacturing Conference
Reviewed Paper

THE EFFECT OF PROCESS PARAMETERS AND MECHANICAL PROPERTIES OF DIRECT ENERGY DEPOSITED STAINLESS STEEL 316

Mojtaba Izadi[*], Aidin Farzaneh[*], Ian Gibson[*], Bernard Rolfe[*]

[*]School of Engineering, Deakin University, Geelong, Victoria, Australia

Abstract

Process parameters in Direct Energy Deposition (DED) Additive Manufacturing are playing an important role in order to fabricate desired parts. In this research, we studied the effect of 3 process parameters, namely laser power, scan speed and powder feed rate. Based on variation of these parameters, we examined macrostructure and mechanical properties of stainless steel 316 fabricated parts, employing an orthogonal L9 array using the Taguchi technique. The results showed laser power to be the most effective factor whereas scan speed and powder feed rate were respectively less effective. In addition, effect of height of deposition was also considered. The results indicated change in macrostructure with increasing height. Finally, validation of a previously defined energy density equation for the DED process was studied. The results clearly showed the current energy density equation cannot fully represent a relation between input energy and output geometry, macrostructure, and mechanical properties.

Introduction

Additive Manufacturing (AM) is a relatively new method of fabrication that is being implemented widely in automotive, medical, aerospace industries [1]. Metal-based AM is increasing at a particularly high rate, focusing on direct manufacture of complex geometry metal parts. Control of process parameters in order to achieve desired mechanical property, macrostructure, microstructure, and dimensional accuracy has been always a challenge on Direct Energy Deposition metal AM processes in particular [2]. Laser Engineered Net Shaping (LENS^{TM}) is a typical process of Direct Energy Deposition and the subject of this research. In this specific process, there are up to four nozzles that deposit powders and a laser which melts this powder to create a melt pool in order to fabricate or repair a metallic part on a substrate [3].

To address these problems, firstly it is necessary to have an understanding of the effect of parameters on part properties. In order to reach that goal, Kobryn et al studied the effect of laser power, scan speed, and substrate thickness on porosity for Ti-6Al-4V (Ti6-4) deposits. They found porosity declines with increasing laser power [4]. Krishna et al fabricated several cylindrical titanium samples with different dimensions, and different values of open and close pores with random process parameters such as laser power, scan speed, powder feed rate and hatch distance. They reported compressive strength changes by changing the mentioned process parameters [5]. With the same methodology, Bandyopadhyay et al deposited several samples with different materials such as pure Ti and TiNi alloy and then compared compressive stiffness of samples that have similar porosity[6]. They showed compressive stiffness for NiTi samples are much lower. The main drawback of these studies is that all process parameters were chosen randomly. Two further studies, one using pure titanium and one using Ti6-4, were carried out on the effect of porosity distribution on mechanical properties. The result clearly indicated pore distribution is very important on mechanical property for both materials [7, 8].

In order to overcome the problem of random parameter selection, Krishna et al, used a systematic method to fabricate NiTi cylindrical samples, studying each process parameter individually. They varied one parameter and kept the rest constant. This raises a question, what is the effect of a combination of parameter variations on porosity? To tackle this issue, they employed total energy input per volume of each scan (E), called energy density equation, which is based on Powder Based Systems (PBS). PBS researchers have found a reasonable relation between energy density and mechanical properties such as density, hardness, wear resistance as well as resulting macrostructure [9-12]. This energy density equation includes laser power (P), scan speed (v), hatch distance or scan line spacing (h) and layer thickness (t) to unify these parameters [13] ;

$$E = P/v \times h \times t \quad (1)$$

Ferguson et al. investigated scan speed and powder feed rate while laser power was constant to create an empirical solution. They presented a new unification unit named linear mass density, dm/dl (g/mm), which includes laser scan speed and powder feed rate. The aim of this study was to obtain the closest parameter combination to create a non-porous bulk structure over each $cm^3$of stainless steel 420 or steel 4140. However, in the mentioned study, mechanical properties were not analysed[14].

There are also numerous studies investigating the effect of several random process parameters on porosity for different materials by depositing cylindrical samples and machining them to make standard fatigue or tensile samples [15-17]. The main disadvantages of this approach are that there is no guarantee of a homogeneous distribution of porosity on these samples. Porosity is likely to vary in such samples due to uneven heat distribution from the bottom to top. As explored by Manvatkar et al. by increasing the number of layers in a thin wall made of stainless steel 316, wall cooling rate decreases; whereas maximum temperature greatly increases. Microhardness tests in this study showed hardness decreases by increasing height [18]. Interestingly Amine et al. indicated value of hardness in lower layers is higher than the upper layers for Stainless steel 316L in multilayers of thin wall, in another word, hardness decreases at increasing heights [19]. However, Yan et al. found different results for Ti6-4. They indicated that hardness increases as you measure higher up the part [20].

In this paper, firstly the relationship between energy density and outputs such as geometry, porosity, and mechanical properties will be studied. Secondly, effect of height on macrostructure also will be investigated. Finally, effect of porosity on mechanical properties will be explored.

Material and Methods

In this study, experimental design based on L9 orthogonal array of Taguchi method is used and three process parameters in three levels; low, mid and high, are investigated. Each level is constant in 3 samples while the other 2 are changed. As this study is done to find any potential effect of process parameters on porosity, there was no repetition to validate the results and further study should be done with more samples to calculate the variance. Stainless steel 316 with spherical particle size between 50 to 150 µm was deposited on a substrate of the same material and dimensions of 125mm×125mm×25mm. A Laser Engineered Net Shaping (LENS^{TM}) MR7 (Optomec Inc. Albuquerque, NM) machine was used to build the samples. Input layer thickness and hatch distance were 0.254 and 0.381 mm respectively. In addition, laser focal distance was 9.652 mm. All nine cylindrical specimens were manufactured in a glove box containing Argon atmosphere with O_2 content less than 10 ppm to minimize oxidation during the deposition process. It should be mentioned that each cylinder was

fabricated individually, and after each fabrication there was an approximate 10 minutes pause time to let the substrate cool down to normal temperature.

Process parameter variations can be seen from Table 1. After part fabrication, dimensions for all parts, by employing micro-scope and Vernier calipers, were measured. Then porosity for the top and bottom each sample was measured using ImageJ 2D software, following removal of the top material to maintain an equal sample height. Finally, compression test in order to measure compressive stiffness was carried out using Instron 50KN.

Table1. Process parameters and energy density

Specimen	Laser power(W)	Scan speed(mm/s)	Powder feed rate (gram/min)	Energy density (J/mm^2)
L1	250	8.5	7.0	305.12
L2	250	12.7	10.0	203.41
L3	250	17.0	13.5	152.55
L4	200	8.5	10.0	244.09
L5	200	12.7	13.5	162.73
L6	200	17.0	7.0	122.05
L7	150	8.5	13.5	183.07
L8	150	12.7	7.0	122.05
L9	150	17.5	10.0	91.54

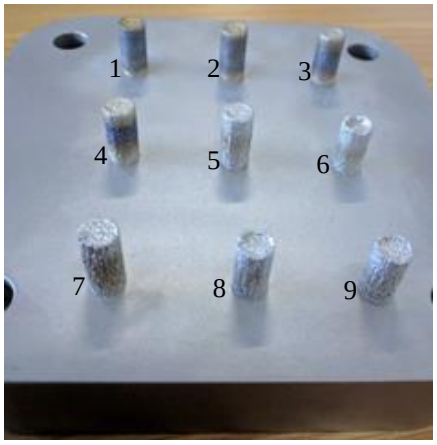

Figure1. Samples as deposited

Results and discussions

In this section, the relationship between energy density and dimension, porosity and mechanical properties are studied. Then, the effect of height on porosity will be investigated. Finally, the effect of process parameters on compressive stiffness will be considered.

Energy Density and Dimension

Different process parameters produce different results in the final cylinders' dimensions. The initial target for dimensions was 6.5mm Ø and 14mm length. These dimensions were chosen so that we could trim the samples by using wire cut, and make them 13mm length as a scaled dimension according to ASTM Standard E9-09 [21]. However, none of the samples were fabricated with the targeted dimensions. Part fabrication dimensions are shown in Table 2. This low accuracy seems due to two reasons. One could be related to process parameters unable to create a proper melt pool. Another reason may be a cumulative effect

caused by the build strategy used where the outline of the part is deposited, followed by a fill pattern. This issue can be seen more on L6 and L8 (Figure 1), where lack of powder infill is significant.

As can be seen from Table 2, there is no specific trend between energy density (as computed using Equation 1) and dimension. For instance, in L1 and L4, average length increases by decreasing energy density, while in L7 and L9 average length increases by increasing energy density. More interestingly L6 and L8, which have exactly the same energy density, average length is very different (see Figure 2A). Also, the diameter of cylinders is slightly different from bottom and top. Similarly, there is no logical relationship between average diameter of top and bottom and energy density (see Figure 2B). In both figures, volumes are normalized between 0-1 in order to show correlation between energy density and dimensions.

Table2. Energy density and dimensional variations

Specimen	Energy density (J/mm^2)	Length on edges (mm)	Length on centre(mm)	Ave length (mm)	Diameter on bottom (mm)	Diameter on top (mm)	Ave Diameter (mm)
L1	305.12	14.65	14.30	14.48	7.28	7.14	7.21
L2	203.41	14.56	14.42	14.49	7.28	7.14	7.21
L3	152.55	14.58	14.38	14.48	7.24	7.14	7.19
L4	244.09	14.70	14.49	14.60	7.24	7.01	7.12
L5	162.73	14.67	14.55	14.61	7.20	6.85	7.02
L6	122.05	12.87	10.94	11.91	7.10	6.84	6.97
L7	183.07	15.20	15.05	15.13	7.21	6.92	7.07
L8	122.05	13.25	12.19	12.72	6.92	6.69	6.80
L9	91.54	13.43	12.63	13.03	7.06	6.98	7.02

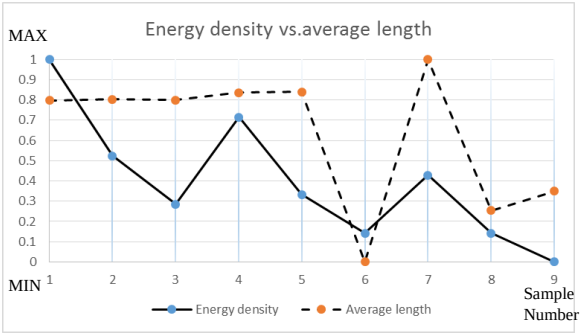

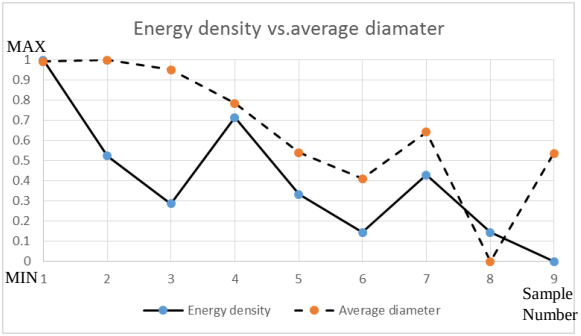

Figure 2. A) Energy density vs. average length B) Energy density vs. average diameter

Energy density and Porosity

In DED there are several types of pores. Lack of fusion porosity; caused by insufficient/incomplete melting which highly depends on input parameters. Gas porosity; caused by entrapment of gas from the powder feed system and/or gas released from the powder particles. Finally, hatch distance porosity; structure which is created by increasing hatch spacing between two cross-sectional layers [22, 23].

Volume of porosity is different in each of the build samples, but there is no apparent relationship between energy density and amount of porosity as seen in Table 3 and Figure 3.

Table3. Energy density and average porosity

Specimen	Energy density (J/mm^2)	Ave Porosity (%)
L1	305.12	1.18
L2	203.41	1.77
L3	152.55	2.10
L4	244.09	2.98
L5	162.73	5.96
L6	122.05	6.67
L7	183.07	15.49
L8	122.05	15.11
L9	91.54	15.82

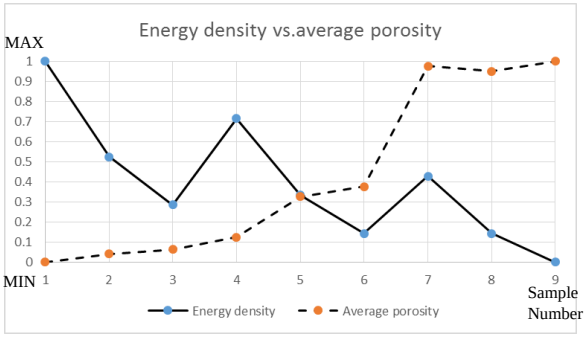

Figure 3. Relation between energy density and average porosity

Energy Density and Mechanical Properties

We also studied the relationship between the energy density and compressive stiffness. In this case, although a trend between energy densities of samples and compressive stiffness can be seen, energy density figures could not be used to determine the exact compressive stiffness (see Table 4 and Figure 4).

Table4. Energy Density and mechanical properties

Specimen	Energy density (J/mm2)	Compressive stiffness (GPa)
L1	305.12	520
L2	203.41	310
L3	152.55	271
L4	244.09	380
L5	162.72	120
L6	122.05	124
L7	183.07	118
L8	122.05	71
L9	91.54	63

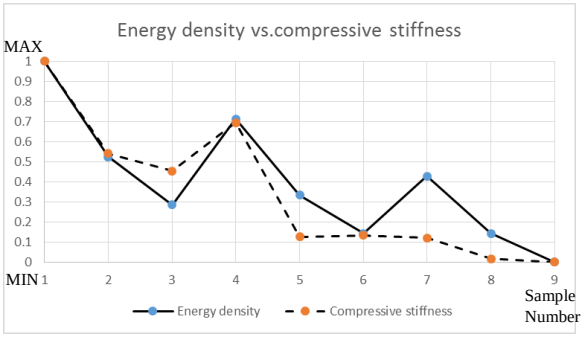

Figure 4. Relationship between Energy density and Mechanical properties

Mechanical Properties and Porosity

In order to understand the effect of porosity on mechanical property, compression tests were carried out on the samples. The sample sizes were not standard according to ASTM, which may have resulted in a measurement error in L1 which has an unusual 520GPa value for stiffness. However, it is considered that they still can be compared against each other. The error may be due to the close strain control points during the test and so could be avoided by using longer specimens in future. The trend of results clearly shows by increasing porosity, compressive stiffness decreases. However, there are two exceptions. Specimen number 4 has higher porosity compared with L2 and L3, but it also has higher compressive stiffness. In addition, specimen number 7 has higher porosity than L8 and also has higher compressive stiffness. This could be the effect of grain sizes or pore distribution. These assumptions should be validated in future by microscopic evaluation of grain size and the more comprehensive use of ImageJ 2D to find the pore distributions.

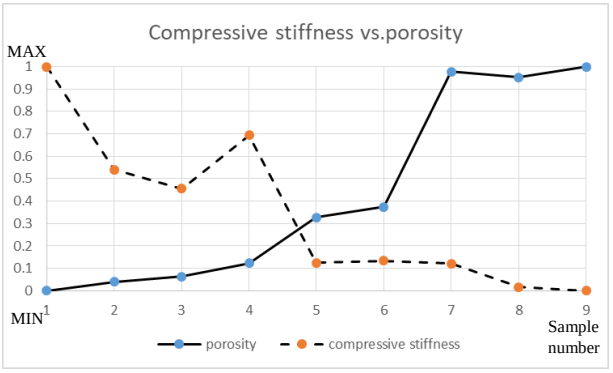

Figure 5. Relation between and average porosity volume and compressive stiffness

Table 5. Relation between Porosity volume and Compressive stiffness (Gp)

Specimen	Porosity on bottom (%)	Porosity on top (%)	Average porosity (%)	Compressive Stiffness (GPa)
L1	1.85	0.51	1.18	520
L2	2.61	0.92	1.77	310
L3	2.57	1.62	2.10	271
L4	3.54	2.41	2.98	380
L5	8.05	3.86	5.96	120
L6	6.52	6.81	6.67	124
L7	15.87	15.11	15.49	118
L8	17.12	13.10	15.11	71
L9	17.92	13.71	15.82	63

Height and Porosity

In deposited samples, it is seen that there is more porosity on the bottom than near the top in most cases (see Figure 6 and 7). This is likely due to high cooling rate on layers which are close to the substrate (see Table 5). However, sample number L6 is an exception. This sample was observed to be the shortest sample and therefore possibly there was insufficient powder for each layer and the laser was therefore possibly remelting previous layers and thus increasing density (see Figure 8).

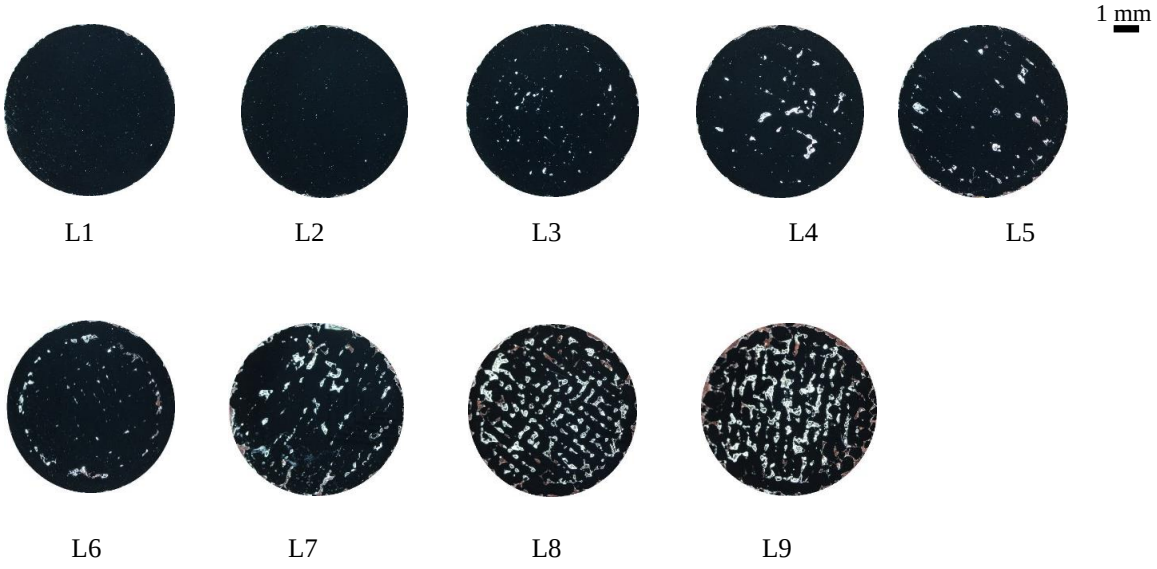

Figure 6. Bottom of specimens

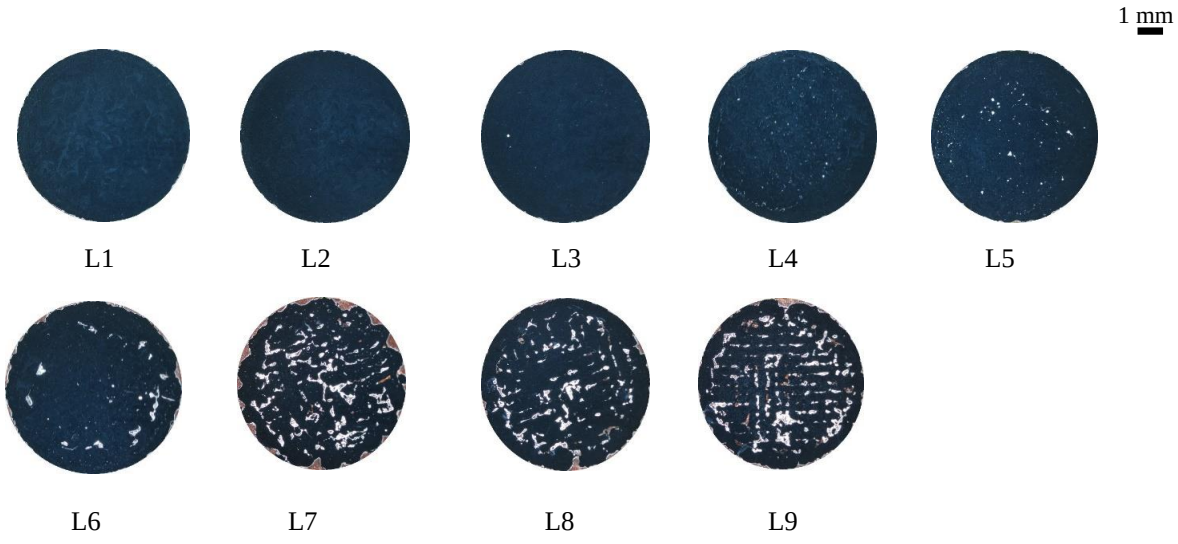

Figure 7. Top of the specimen

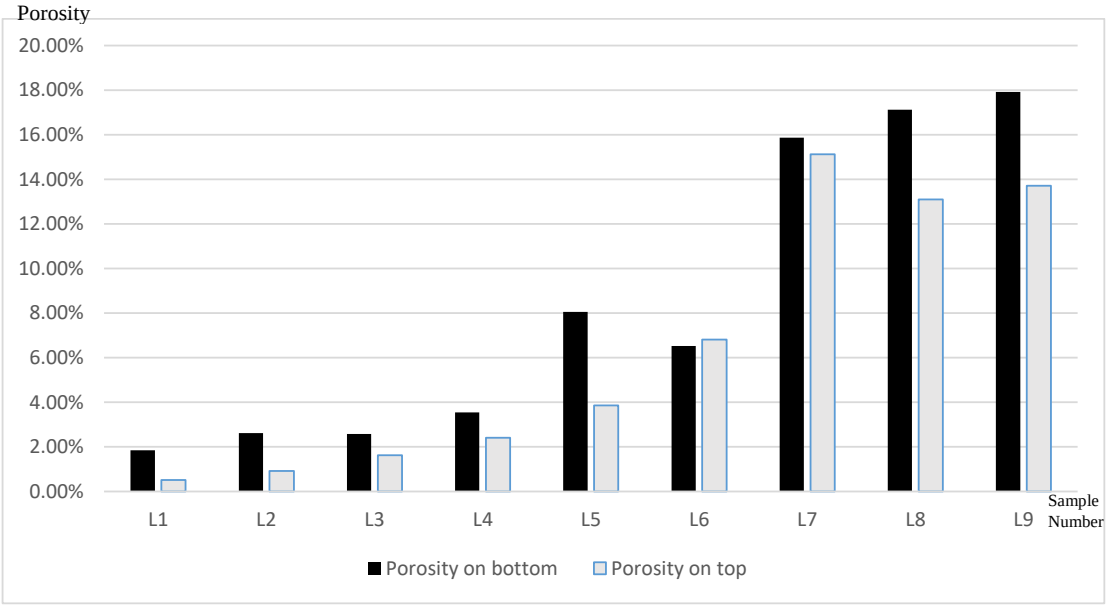

Figure 8. Porosity on bottom and top

Effect of process parameters on porosity

Different process parameters have different effects on porosity. Laser power by rank 1 has the largest effect on porosity. Scan speed and powder feed rate stand on second and third rank respectively (See Table 6). These ranks are obtained through Minitab statistical analysis software.

Table6. Ranking effect of process parameter on bottom porosity

Level	Laser power	Scan speed	Feed rate
1	16.972	7.086	8.498
2	6.038	9.262	8.025
3	2.344	9.006	8.831
Rank	1	2	3

DOE Results validation

The means for each level are considered as the average of the response achieved at the same control factor levels in a static Taguchi DOE (see Table 6). The analysis of means of the experiment show which parameters have more influence on density.

S/N ratios evaluate the effect of noise, which is a measure of the process robustness, of the response to variability of a parameter's influence. The general nature of this graph is the same as the means effect (see Figure 9).

In order to check the validity of the results from the DOE, mean effect graph for means and signal to noise (S/N) ratio should be considered. The lowest values for each factor in Means plots should be equal to the highest value of S/N ratio which can be seen in fig 9. Hence, these graphs indicate the DOE is validated.

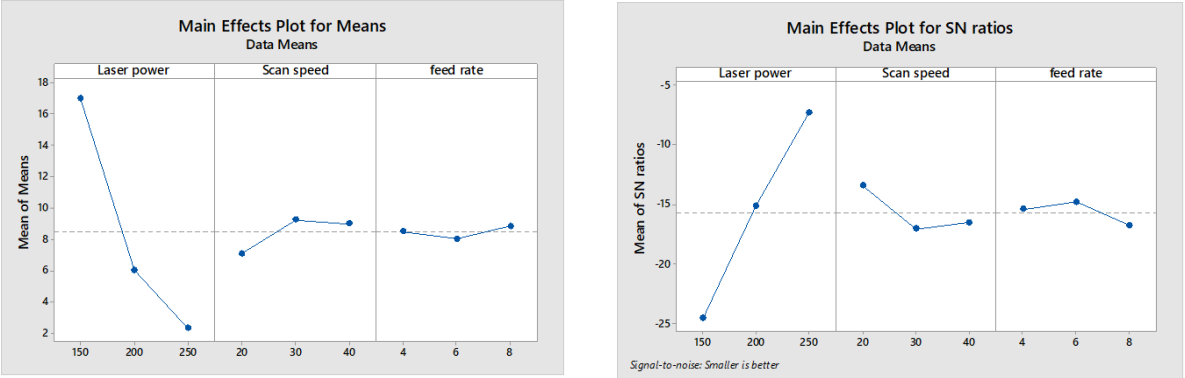

Figure 9. Means vs. SN ration for bottom porosity

Conclusion

By increasing the height, the amount of porosity in general decreases, probably due to decreasing cooling rate on top layers. This also affects mechanical properties. Hence, there is a need to control the macrostructure, and consequently mechanical properties, in order to achieve a homogeneous structure. In addition, according to the results, there is difficulty in finding a correlation between energy density and outputs. It is likely that the energy density equation is incorrect for DED. This could be improved by including parameters relating to powder feed rate, thermal transfer properties, and height above the substrate, etc. These results certainly indicate that energy density calculation in DED is more complex than for powder bed, and perhaps could be replaced by a function that presents a logical correlation between input parameters and outputs.

References

[1] I. Campbell, D. Bourell, and I. Gibson, "Additive manufacturing: rapid prototyping comes of age," *Rapid Prototyping Journal*, vol. 18, pp. 255-258, 2012.

[2] G. Sun, R. Zhou, J. Lu, and J. Mazumder, "Evaluation of defect density, microstructure, residual stress, elastic modulus, hardness and strength of laser-deposited AISI 4340 steel," *Acta Materialia*", vol. 84, pp. 172-189, 2015.

[3] Y. Zhai, H. Galarraga, and D. A. Lados, "Microstructure, static properties, and fatigue crack growth mechanisms in Ti-6Al-4V fabricated by additive manufacturing: LENS and EBM," *Engineering Failure Analysis*, 2016.

[4] P. A. Kobryn, E. H. Moore, and S. L. Semiatin, "The effect of laser power and traverse speed on microstructure, porosity, and build height in laser-deposited Ti-6Al-4V," *Scripta Materialia*, vol. 43, pp. 299-305, 7/28/ 2000.

[5] B. V. Krishna, S. Bose, and A. Bandyopadhyay, "Low stiffness porous Ti structures for load-bearing implants," *Acta Biomaterial*, vol. 3, pp. 997-1006, 2007.

[6] A. Bandyopadhyay, B. V. Krishna, W. Xue, and S. Bose, "Application of Laser Engineered Net Shaping (LENS) to manufacture porous and functionally graded structures for load bearing implants," *Journal of Materials Science: Materials in Medicine*, vol. 20, pp. 29-34, 2008.

[7] V. K. Balla, S. Bose, and A. Bandyopadhyay, "Understanding compressive deformation in porous titanium," *Philosophical Magazine*, vol. 90, pp. 3081-3094, 2010.

[8] S. Roy, N. Khutia, D. Das, M. Das, V. K. Balla, A. Bandyopadhyay, *et al.*, "Understanding compressive deformation behavior of porous Ti using finite element analysis," *Materials Science and Engineering C: Biomimetic and Supramolecular Systems*, vol. 64, pp. 436-443, 2016.

[9] W. Di, Y. Yongqiang, S. Xubin, and C. Yonghua, "Study on energy input and its influences on single-track, multi-track, and multi-layer in SLM," *The International Journal of Advanced Manufacturing Technology*, vol. 58, pp. 1189-1199, 2012.

[10] H. Gu, H. Gong, D. Pal, K. Rafi, T. Starr, and B. Stucker, "Influences of energy density on porosity and microstructure of selective laser melted 17-4PH stainless steel," in *2013 Solid Freeform Fabrication Symposium*, 2013, p. 474.

[11] Q. Jia and D. Gu, "Selective laser melting additive manufacturing of Inconel 718 superalloy parts: Densification, microstructure and properties," *Journal of Alloys and Compounds*, vol. 585, pp. 713-721, 2014.

[12] B. Vandenbroucke and J.-P. Kruth, "Selective laser melting of biocompatible metals for rapid manufacturing of medical parts," *Rapid Prototyping Journal*, vol. 13, pp. 196-203, 2007.

[13] B. V. Krishna, S. Bose, and A. Bandyopadhyay, "Fabrication of Porous NiTi Shape Memory Alloy Structures Using Laser Engineered Net Shaping," *Journal of biomadical Materials Researche Part B-Applied Biomaterial*, vol. 89B, pp. 481-490, 2009.

[14] J. B. Ferguson, B. F. Schultz, A. D. Moghadam, and P. K. Rohatgi, "Semi-empirical model of deposit size and porosity in 420 stainless steel and 4140 steel using laser engineered net shaping," *Journal of Manufacturing Processes*, vol. 19, pp. 163-170, 2015.

[15] S. Bernard, V. K. Balla, S. Bose, and A. Bandyopadhyay, "Rotating bending fatigue response of laser processed porous NiTi alloy,"Materials Science & Engineering C-Material for Biological Application, vol. 31, pp. 815-820, 2011.

[16] A. Yadollahi, N. Shamsaei, S. M. Thompson, and D. W. Seely, "Effects of process time interval and heat treatment on the mechanical and microstructural properties of direct laser deposited 316L stainless steel," *Materials Science & Engineering: A*, vol. 644, pp. 171-183, 2015.

[17] A. J. Sterling, B. Torries, N. Shamsaei, S. M. Thompson, and D. W. Seely, "Fatigue behavior and failure mechanisms of direct laser deposited Ti–6Al–4V," *Materials Science & Engineering: A*, vol. 655, pp. 100-112, 2016.

[18] V. Manvatkar, A. Gokhale, G. Jagan Reddy, A. Venkataramana, and A. a. i. a. i. De, "Estimation of Melt Pool Dimensions, Thermal Cycle, and Hardness Distribution in the Laser-Engineered Net Shaping Process of Austenitic Stainless Steel," *Metallurgical & Materials Transactions. Part A*, vol. 42, pp. 4080-4087, 12/15/ 2011.

[19] T. Amine, J. Newkirk, and F. Liou, "An investigation of the effect of laser deposition parameters on characteristics of multilayered 316 L deposits," *International Journal of Advanced Manufacturing Technology*, vol. 73, pp. 1739-1749, 2014.

[20] L. Yan, X. Chen, W. Li, J. Newkirk, and F. Liou, "Direct laser deposition of Ti-6Al-4V from elemental powder blends," *Rapid Prototyping Journal*, vol. 22, pp. 810-816, 2016.

[21] "Standard Test Methods of Compression Testing of Metallic Materials at Room Temperature," ed: ASTM International, 2009.

[22] B. V. Krishna, S. Bose, and A. Bandyopadhyay, "Laser Processing of Net-Shape NiTi Shape Memory Alloy," *Metallurgical & Materials Transactions. Part A*, vol. 38, pp. 1096-1103, 05// 2007.

[23] J. Kummailil, C. Sammarco, D. Skinner, C. A. Brown, and K. Rong, "Effect of Select LENS™ Processing Parameters on the Deposition of Ti-6Al-4V," *Journal of Manufacturing Processes*, vol. 7, pp. 42-50, // 2005.